



2004

Classical Stern-Gerlach profiles of Mn5 and Mn6 clusters

N. O. Jones

Virginia Commonwealth University

Shiv N. Khanna

Virginia Commonwealth University, snkhanna@vcu.edu

Tunna Baruah

Naval Research Laboratory

M. R. Pederson

Naval Research Laboratory

Follow this and additional works at: http://scholarscompass.vcu.edu/phys_pubs

 Part of the [Physics Commons](#)

Jones, N.O., Khanna, S.N., Baruah, T., et al. Classical Stern-Gerlach profiles of Mn5 and Mn6 clusters. *Physical Review B*, 70, 045416 (2004). Copyright © 2004 American Physical Society.

Downloaded from

http://scholarscompass.vcu.edu/phys_pubs/98

This Article is brought to you for free and open access by the Dept. of Physics at VCU Scholars Compass. It has been accepted for inclusion in Physics Publications by an authorized administrator of VCU Scholars Compass. For more information, please contact libcompass@vcu.edu.

Classical Stern-Gerlach profiles of Mn_5 and Mn_6 clusters

N. O. Jones and S. N. Khanna

Physics Department, Virginia Commonwealth University Richmond, Virginia 23284-2000, USA

Tunna Baruah and M. R. Pederson

Center for Computational Materials Science, Naval Research Laboratory, Washington, D.C. 20375-5345, USA

(Received 26 January 2004; published 23 July 2004)

Mn_5 and Mn_6 clusters have recently been found to exhibit Stern-Gerlach profiles marked by a central peak that broadens with the increasing field gradient. The profiles neither exhibit a reminiscence of space quantization as observed through a splitting of beams for the case of free atoms, nor a net deflection characteristic of superparamagnetic relaxations observed in other transition metal clusters. It is proposed that this new behavior results from a weak coupling of localized atomic moments. *ab initio* electronic structure studies are carried out to show that a Mn_5 cluster has isomers with spin magnetic moments of $3 \mu_B$, $13 \mu_B$, and $23 \mu_B$ while a Mn_6 cluster has isomers with moments of $2 \mu_B$, $8 \mu_B$, $16 \mu_B$, and $26 \mu_B$, respectively. The isomers can be obtained by sequential turning of the local atomic moments starting from the ferromagnetic state and can be seen in the negative ion photoelectron spectra of the anions. The weak coupling of the atomic moments, however, leads to unconventional spin dynamics that result in classical broadening of the Stern-Gerlach profiles and lower apparent magnetic moments. The theoretical results illustrate how a combination of the negative ion photodetachment spectroscopy and Stern-Gerlach profiles can provide information on the net spin moment, interatomic spin coupling, and spin dynamics.

DOI: 10.1103/PhysRevB.70.045416

PACS number(s): 73.22-f, 71.15.Nc, 31.15.Ar

I. INTRODUCTION

Atomic clusters constitute a new phase of matter intermediate between atoms and solids. Consequently, they exhibit novel features that are distinct from the atoms or solids.¹ In particular, the magnetic properties of clusters are truly unique.² The magnetic moments of clusters are traditionally measured using the Stern-Gerlach setup that was used to demonstrate space quantization, almost 80 years ago. Here, a beam of particles is passed through a gradient magnetic field that tries to orient the moments as well as deflect them. For atoms with total angular momentum J , the ensuing beam splits into $2J+1$ components [see Fig. 1(a)]. This well-known experiment inspired the first experimental measurements³ of the magnetic moment of small free Fe_n and subsequently⁴ Co_n and Ni_n clusters. It was thought that as in the case of atoms, the beam would split into $2J+1$ components and that one could determine the magnetic moment through the number of subbeams. The actual experiments [Fig. 1(b)], however, showed that all the clusters in the beam undergo a uniform deflection. Further, the calculated magnetization per atom was far less than the moment per atom in solids contrary to theoretical predictions that the clusters would have higher magnetic moments than the corresponding bulk solids. Khanna and Linderoth⁵ explained this behavior as due to superparamagnetic relaxations. They argued that the atomic spins in these clusters were strongly coupled and that the cluster behaved like a giant magnet with a moment that is the sum of atomic moments. They further argued that the magnetic anisotropy in reduced sizes was much less than the cluster temperatures. As in case of free atoms, the spin moment of clusters entering the magnetic field undergo precessions around the field. However, unlike

the case of free atoms, the clusters also have a finite angular momentum associated with the rotational motions and by coupling to the cluster angular momentum via a spin-orbit like coupling, the total spin of the free clusters can relax in space. The clusters therefore behave like giant atoms undergoing superparamagnetic relaxations, leading to a uniform deflection. Over the past years, this model has been extensively used to interpret the experimental data.⁶ Later experiments⁷ on Gd_n and in particular on Gd_{21} did provide cases where the beam spreads asymmetrically around the zero deflection [Fig. 1(c)]. This arises when the anisotropy is larger than the cluster rotational temperatures and leads to what is termed as “locked moment behavior.”

The known behaviors of the Stern-Gerlach profiles can then be summarized under three categories as schematically shown in Fig. 1: (1) Splitting of the beam into $2J+1$ components observed in free atoms, (2) a net uniform deflection observed in Fe_n , Co_n , and Ni_n clusters,³ and (3) asymmetric broadening as observed in Gd_n clusters due to high magnetic anisotropy that leads to blocking of the magnetic moment in certain directions.⁴ Recent Stern-Gerlach experiments⁸ [see Fig. 1(d)] on Mn_5 and Mn_6 , however, exhibit profiles that fit neither of the known patterns. The observed deflection profiles correspond to a relatively broad symmetric central peak without any net deflection. Further, the broadening increases as one increases the gradient field. The absence of splitting and a net deflection excludes the categories (1) and (2). As we will show, the magnetic anisotropies in these clusters are much lower than the experimental temperatures. This excludes the locked moment behavior as in Gd_{21} .

What is even more surprising is that our *ab initio* studies indicate that the magnetic anisotropy in small Mn_n clusters are generally smaller than the rotational temperatures making them as potential candidates for superparamagnetic relax-

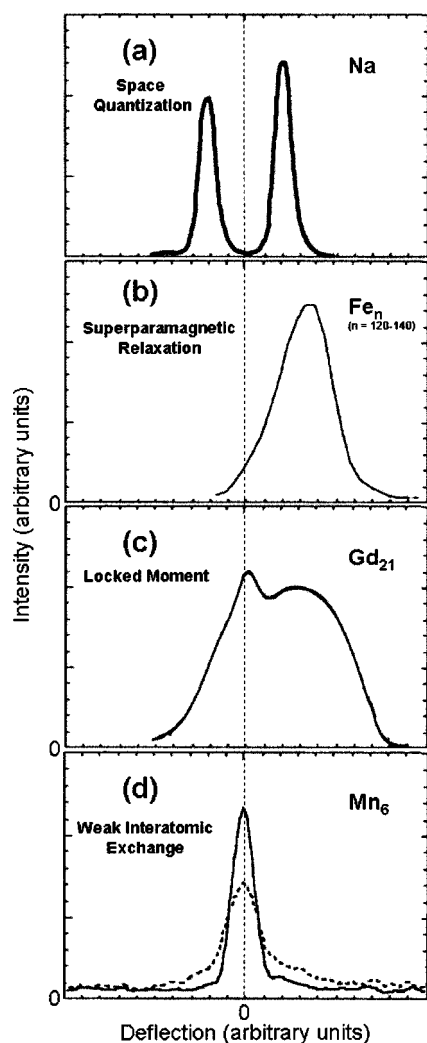


FIG. 1. Schematic Stern-Gerlach profiles for (a) Na atoms (b) Fe_n ($n=120-140$) clusters (Ref. 3) and (c) Gd_{21} clusters (Ref. 4) Fig. (d) shows the spatial profile for Mn_6 clusters (Ref. 8) recorded with $\partial B/\partial Z=0$ (solid line) and with $\partial B/\partial Z=192 \text{ T m}^{-1}$ (dashed curve).

ations. Indeed, experiments on clusters containing seven Mn atoms⁶ show superparamagnetic relaxations and hence uniform deflections. Why are Mn_5 and Mn_6 so different? In this work, we show that this new behavior arises due to a weak interatomic exchange coupling that makes them behave like an assembly of weakly correlated atomic spins and leads to several magnetic isomers. We show that the ground state of Mn_5 has isomers with spin multiplicity of 4, 14, and 24, respectively, while the ground state of Mn_6 has isomers with multiplicity of 3, 9, 17, and 27, respectively. By comparing the calculated spectra for the anions with the negative-ion photodetachment spectra,⁹ we prove that these isomers are indeed present in beams. However, the weak intraatomic exchange coupling leads to new spin dynamics that lead to centrally peaked deflection profiles and lower observed magnetic moments in Stern-Gerlach experiments.

It is interesting to briefly review the behavior of Mn in bulk and in reduced sizes. Bulk Mn does not crystallize into fcc, bcc, or hcp lattices but has a α Mn structure¹⁰ with a

large unit cell of 58 atoms and is antiferromagnetic (AF). Electron-spin resonance (ESR) (Ref. 11) and absorption spectrum¹² studies indicate that Mn_2 molecule exists in a van der Waal (VdW) AF state like the bulk antiferromagnetic structure. ESR studies on larger Mn_n clusters¹³ in a matrix, however, observe a ferromagnetically coupled cluster with a moment of $25\mu_B$. The cluster with this large moment contained more than four Mn atoms and it was suggested that it could be a Mn_5 . There have been numerous theoretical studies^{14,15} on small Mn_n clusters containing 2–8 atoms. These studies mostly focused on ferromagnetic solutions and free Mn_2 , Mn_3 , and Mn_4 are proposed to be ferromagnetic with total moments of $10\mu_B$, $15\mu_B$ and $20\mu_B$, respectively. For Mn_5 , the earlier studies predict a moment between $23\mu_B$ and $25\mu_B$ and for Mn_6 a moment of $26\mu_B$. These studies did not examine the antiferromagnetic configurations and hence missed the existence of isomers.

In Sec. II we describe the details of our method while Sec. III is devoted to a discussion of results. Finally, Sec. IV contains the conclusions of this work.

II. DETAILS OF CALCULATIONS

The electronic structure calculations of the ground-state geometry and the spin magnetic moment of Mn_5 and Mn_6 were carried out using the first-principles density-functional approach. The molecular orbitals were expressed as a linear combination of atomic orbitals centered at the atomic sites. The matrix elements of the Hamiltonian operator between the molecular orbitals required in a self-consistent solution of the Kohn-Sham equations were carried out numerically on a mesh of points. The actual calculations were carried out using the NRLMOL (Naval Research Laboratory Molecular Orbital Library) set of codes developed by one of the present authors and co-workers.^{16,17} The basis set for Mn consisted of 7s, 5p, and 4d functions constructed from 20 bare Gaussians.¹⁸ The basis set was supplemented by 1d Gaussian. All geometries were optimized fully with Hellmann-Feynman forces smaller than 0.001 hartree/bohr.

For Mn_5 , the investigations covered square pyramid and triangular bipyramid geometrical arrangements. For Mn_6 , we investigated the octahedron, pentagonal pyramid, and trigonal prism structures. No symmetry constraints were imposed to allow maximal variational freedom. In each case, we examined the ferromagnetic and all possible antiferromagnetic configurations. In fact, we first examined the lowest ferromagnetic configuration. We then investigated the changes in energy as individual electronic or atomic spins were turned antiferromagnetically. This was followed by turning various pairs of atomic spins and so on. In each case, the geometry and the spin were optimized starting from reasonable initial values derived from the ferromagnetic solution. The magnetic moments were calculated by integrating the spin density within a sphere surrounding each site. For the criterion for choosing the size of sphere and other numerical details, the reader is referred to the earlier papers.¹⁹

III. RESULTS AND DISCUSSION

The theoretical studies show that the clusters are marked by several energetically low structures. A systematic study of

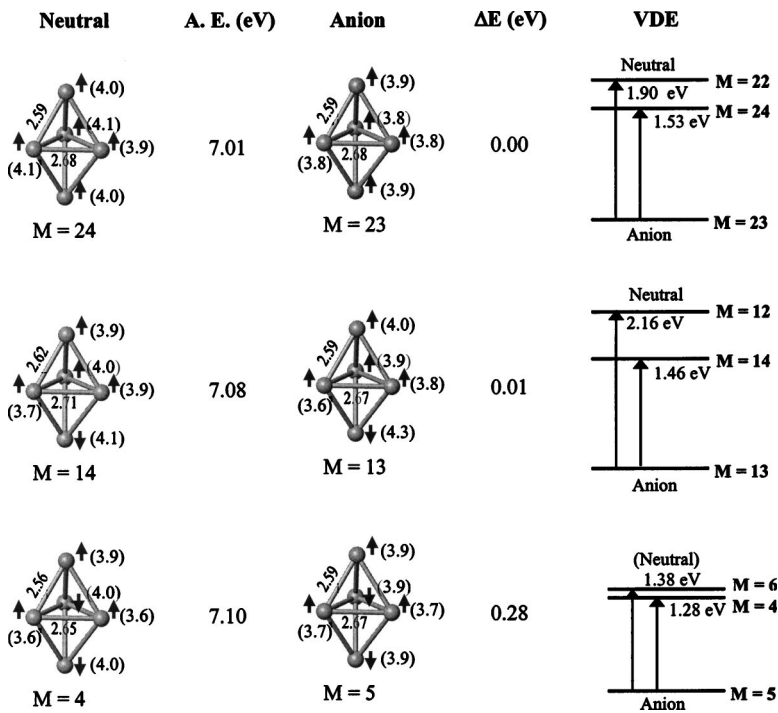


FIG. 2. Ground-state geometry and some of the low-lying isomers for the neutral and anionic Mn₅ clusters. The atomization energy (AE) is given for neutral clusters. For anionic clusters $\Delta E = E - E$ (ground state), representing the energy above the ground state of the anion is also marked. The arrows \uparrow and \downarrow indicate the direction of spin polarization at each site and the corresponding magnetic moments (in μ_B) are given within parenthesis at each site. The bond lengths are in angstrom. Also given are the vertical transition energies from the anion (multiplicity M) to the neutral clusters clusters with multiplicity $M \pm 1$.

the variation of the energy as a function of spin shows that the energy shows minima when the change in spin corresponds to a reversal of the entire atomic spin. This is a signature of the relative strength of the intra-atomic and inter-atomic exchange couplings. In Fig. 2 we show the geometry, spin multiplicity M, the local magnetic moment, and the atomization energies of all the structures within 0.1 eV of the

ground state. The atomization energy AE is defined as

$$AE = [nE(Mn) - E(Mn_n)], \quad (1)$$

where E is the total energy of the respective atoms/clusters. Within the limits of the accuracy of the calculation, these structures can be considered as isomers. For Mn₅, note that the isomers correspond to total spin magnetic moment of

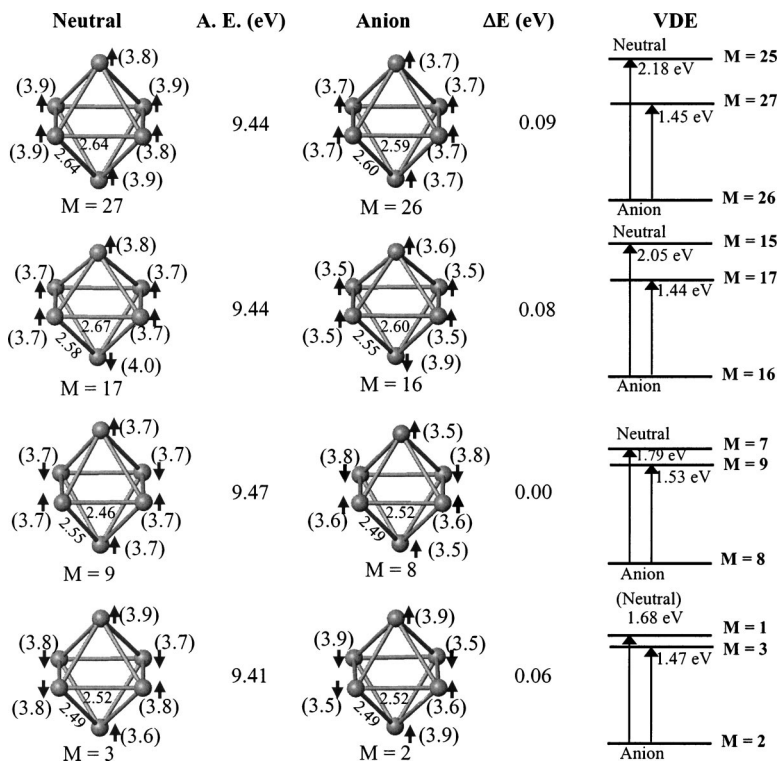


FIG. 3. Ground-state geometry and some of the low-lying isomers for the neutral and anionic Mn₆ clusters. The atomization energy (AE) is given for neutral clusters. For anionic clusters $\Delta E = E - E$ (ground state), representing the energy above the ground state of the anion is also marked. The arrows \uparrow and \downarrow indicate the direction of spin polarization at each site and the corresponding magnetic moments (in μ_B) are given within parenthesis at each site. The bond lengths are in angstrom. Also given are the vertical transition energies from the anion (multiplicity M) to the neutral clusters clusters with multiplicity $M \pm 1$.

$3\mu_B$, $13\mu_B$, and $23\mu_B$. Figure 3 also shows the corresponding ground state and energetically close isomers for Mn_6 . Note that they all correspond to the octahedral structure. The octahedron are, however, marked by slight Jahn-Teller distortions. The isomers now correspond to total spins of $2\mu_B$, $8\mu_B$, $16\mu_B$, and $26\mu_B$. Figures 2 and 3 also show the local magnetic moments at the various sites obtained by integrating the spin charge density within spheres around each site. These are marked within the parenthesis at each site. Note that the atomic magnetic moments around the sites forming the triangular base in Mn_5 are slightly different. This is because the bond lengths in the triangular base are slightly different (it is not an equilateral triangle). Note that all the isomers can be obtained by starting from the ferromagnetic solution and reversing the atomic spins one by one.

Before we proceed further, let us compare our findings with negative-ion photodetachment spectroscopy. Here, a selected cluster anion is crossed with a laser of fixed wavelength and the energy of the photodetached electron is measured. The difference between the energy of the photon and that of the detached electron yields the binding energy of the electron. Now imagine that an anionic cluster has N unpaired electrons and hence a multiplicity $M=N+1$. When the electron is detached, the neutral cluster will have a spin multiplicity of $M-1$ or $M+1$ depending on whether the electron is removed from the majority or the minority state. The peaks in the photodetachment spectra corresponding to the two transitions can be compared with theoretical calculations where one first determines the ground state of the anion including its spin multiplicity and then the energies to make the transition to the neutral states with multiplicity of $M-1$ or $M+1$, with no change in the initial anionic geometry. If the calculated energies agree quantitatively with the experimental peaks, one can conclude that the spin multiplicity calculated in theory must be correct. We had earlier used²⁰ such a procedure to identify the ground state of Fe_3 and Tono *et al.*²¹ have recently used it for the ground state of Cr_2O .

In order to compare with the experimental results on photodetachment experiments we determined the ground-state geometry, spin multiplicity, and binding energy of the Mn_5 and Mn_6 anions by examining all the ferromagnetic and antiferromagnetic configurations. The results are shown in Figs. 2 and 3. For Mn_5 , the ground state of the anion is a ferromagnetic structure with a spin multiplicity of 23. Close to the ground state are the antiferromagnetic configurations with spin multiplicities of 13 and 5. For Mn_6 , the ground state corresponds to $M=8$. In this case, the states with multiplicity of 2, 16, and 26 are only 0.06, 0.08, and 0.09 eV above the ground state. To compare with negative-ion photodetachment data, we examined the vertical transitions to the neutral cluster with a multiplicity one higher and one lower than the anion. These are shown in Figs. 2 and 3. If one only focuses on the absolute ground state, we predict that the spectra of Mn_5 will be marked by peaks at 1.53 and 1.90, respectively, while that of Mn_6 will be marked by 1.53 and 1.79 eV, respectively. In addition to these main peaks, one expects transition around other energies corresponding to isomers. In particular, for Mn_6 , one expects the second transition to be very broad with peaks at 1.68, 1.79, 2.05, and 2.18 eV, respectively. Bowen *et al.*⁹ have recently studied

the negative-ion photodetachment spectra for Mn_5 and Mn_6 . While their detailed spectra will appear in a separate publication, their spectra for Mn_5 show major peaks at 1.5 and 2.0 eV while that of Mn_6 has several close lying peaks around 1.7, 1.8, 2.1, and 2.2 eV. Our predicted peaks are in reasonable agreement with their findings confirming that the isomers are indeed present in the cluster beam. Can one see them in Stern-Gerlach profiles?

As mentioned before, in these experiments, one passes a beam of ferromagnetic clusters through a gradient magnet where the spin magnetic moment interacts with the gradient field to reorient the magnet as well as to displace the clusters laterally. Knickelbein *et al.*⁸ have recently performed such experiments and Fig. 1(d) shows the induced deflection of Mn_6 in the time of flight spectrum. One observes a broadening of the beam as opposed to a net deflection shown by most transition-metal clusters. Further, an increase in the gradient of the magnetic field resulted in an increase of the width of the deflection profile, without net deflection. Figure 2 shows that Mn_5 is marked by isomers with total spin of $3\mu_B$, $13\mu_B$, and $23\mu_B$, respectively. If broadened, these would lead to three separate peaks for multiplicity of 4, 14, and 24 broadened by the gradient in temperature and possible changes in field gradient. While one could argue that the overlap of a large number of peaks could produce a quasiuniform deflection profile, Knickelbein's attempt to fit the profile as a superposition of peaks were not very successful. For the case of broadened peaks, Knickelbein *et al.* were nevertheless able to extract a moment by integrating the area under the peaks. Such a procedure⁸ lead to total cluster moments of $(2-4)\mu_B$ for Mn_5 and Mn_6 . This is far below the average of the total magnetic moment ($13.0\mu_B$) of the isomers given in Figs. 2 and 3. We also calculated the magnetic anisotropy in these clusters using a new approach¹⁹ we have recently developed. The anisotropy energy for Mn_5 and Mn_6 were 7 K and almost 0 K, respectively. The experimental temperatures are more than 50 K. Until now, it has been a mystery as to why clusters with such low anisotropy exhibit no relaxations and why the observed moments are so low.

We believe that the key to this puzzle lies in the strength of interatomic exchanges. As we showed, the energy required to turn an atomic spin in a ferromagnetic cluster is small showing that the atomic spins are not weakly correlated. As the clusters are subjected to the gradient field in a Stern-Gerlach experiment, the spin dynamics resembles that of weakly correlated atomic spins precessing in the magnetic field. Furthermore, in the absence of a central potential, there is no space quantization and the atomic moment exhibits a classical behavior where the cluster is displaced in the up-field or down-field direction depending on the orientation at the entrance in the field gradient. The random orientation of the magnetic moment then leads to a broadening of the beam without any net deflection. The deflection profiles, nevertheless, do broaden as the field gradient is increased and one can integrate the area under the curves to calculate the effective moments.⁸ It is gratifying to note that the calculated cluster magnetic moments using the Stern-Gerlach profiles⁸ in Fig. 1 and a similar one for Mn_5 are indeed around $(2-4)\mu_B$, close to the calculated atomic magnetic moments of $(3.7-4.1)\mu_B$ at a Mn site for Mn_5 and Mn_6 . This shows that the magnetic

moments seen in Stern-Gerlach profiles are really the atomic magnetic moments. The broadening of the profiles and the calculated magnetic moment can thus both be understood within the model.

IV. CONCLUSIONS

To summarize, we have shown how by combining negative ion photodetachment spectroscopy and the Stern-Gerlach magnetic deflection one can obtain information on the ground-state spin multiplicity as well as the strength of interatomic exchange. The ground state of Mn_5 and Mn_6 are marked by magnetic isomers that correspond to different orientations of the atomic spins resulting from the weak interatomic exchange coupling. These isomers can be seen in experiments involving the negative-ion photodetachment spectroscopy. However, they lead to novel spin dynamics in Stern-Gerlach experiments. Here, the weak interatomic exchange results in classical behavior of individual atomic spins. Consequently, the cluster beam merely spreads instead

of undergoing an uniform deflection. We believe that the present paper should also be applicable to other cases such as transition-metal atoms attached to nonmagnetic hosts (such as Mn_5O and Mn_6O). We have just become aware of another work on small Mn_n clusters by Bobadova-Parvanova *et al.*²² who have calculated the magnetic moments of neutral clusters using a similar approach. Our findings on neutral clusters are consistent with their results. These authors, however, did not study the anionic clusters and have not addressed the low observed moments in Stern-Gerlach experiments. Our paper precisely addresses these issues.

ACKNOWLEDGMENTS

S.N.K. and N.O.J. acknowledge partial support from the Department of Energy (Grant No. DE-FG02-96ER45579). T.B. and M.R.P. acknowledge support from ONR (Grant No. N0001400WX2011). The authors are extremely grateful to Dr. M. B. Knickelbein for providing a copy of the experimental Stern-Gerlach Profile and to Dr. K. H. Bowen for sharing his negative-ion photoelectron spectroscopy data.

-
- ¹*Quantum Phenomena in Clusters and Nanostructures*, edited by S. N. Khanna and A. W. Castleman, Jr. (Springer, New York, 2003).
- ²D. D. Awschalom and D. P. Di Vincenzo, *Phys. Today* **48** (4), 43 (1995).
- ³W. A. de Heer, P. Milani, and A. Chatelain, *Phys. Rev. Lett.* **65**, 488 (1990).
- ⁴J. P. Bucher, D. C. Douglass, and L. A. Bloomfield, *Phys. Rev. Lett.* **66**, 3052 (1991).
- ⁵S. N. Khanna and S. Linderoth, *Phys. Rev. Lett.* **67**, 742 (1991).
- ⁶M. B. Knickelbein, *Phys. Rev. Lett.* **86**, 5255 (2001); M. B. Knickelbein, *J. Chem. Phys.* **116**, 9703 (2002).
- ⁷D. C. Douglas, J. P. Bucher, and L. A. Bloomfield, *Phys. Rev. Lett.* **68**, 1774 (1992).
- ⁸M. B. Knickelbein (private communication).
- ⁹K. H. Bowen, International Materials Research Congress 2002, (Cancun, Mexico, Aug. 25–29, 2002 p. 6); K. H. Bowen (private communication).
- ¹⁰R. S. Tebble and D. J. Craik, *Magnetic Materials* (Wiley, New York, 1969), p. 48.
- ¹¹R. J. Van Zee, C. A. Baumann, and W. Weltner, *J. Chem. Phys.* **74**, 6977 (1981).
- ¹²K. D. Bier, T. L. Haslett, A. D. Kirkwood, and M. Moskovits, *J. Chem. Phys.* **89**, 6 (1988).
- ¹³C. A. Baumann, R. J. Van Zee, S. V. Bhat, and W. Weltner, Jr., *J. Chem. Phys.* **78**, 190 (1983).
- ¹⁴M. R. Pederson, F. Reuse, and S. N. Khanna, *Phys. Rev. B* **58**, 5632 (1998).
- ¹⁵S. K. Nayak and P. Jena, *Chem. Phys. Lett.* **289**, 473 (1998).
- ¹⁶M. R. Pederson and K. A. Jackson, *Phys. Rev. B* **41**, 7453 (1990).
- ¹⁷K. A. Jackson and M. R. Pederson, *Phys. Rev. B* **42**, 3276 (1990).
- ¹⁸D. V. Porezag and M. R. Pederson, *Phys. Rev. A* **60**, 2840 (1999).
- ¹⁹M. R. Pederson and S. N. Khanna, *Phys. Rev. B* **59**, R693 (1999).
- ²⁰G. L. Gutsev, S. N. Khanna, and P. Jena, *Phys. Rev. B* **62**, 1604 (2000).
- ²¹K. Tono, A. Terasaki, T. Ohta, and T. Kondow, *Phys. Rev. Lett.* **90**, 133402 (2003).
- ²²P. Bobadova-Parvanova, K. A. Jackson, S. Srinivas, and M. Horoi, *Phys. Rev. A* **67**, 061202(R) (2003).